(2)

ARMY RESEARCH LABORATORY

The XNOVAKTC Rheological Model

Paul J. Conroy

ARL-MR-47 March 1993

NOTICES

Destroy this report when it is no longer needed. DO NOT return it to the originator.

Additional copies of this report may be obtained from the National Technical Information Service, U.S. Department of Commerce, 5285 Port Royal Road, Springfield, VA 22161.

The findings of this report are not to be construed as an official Department of the Army position, unless so designated by other authorized documents.

The use of trade names or manufacturers' names in this report does not constitute indorsement of any commercial product.

DISCLAIMER NOTICE

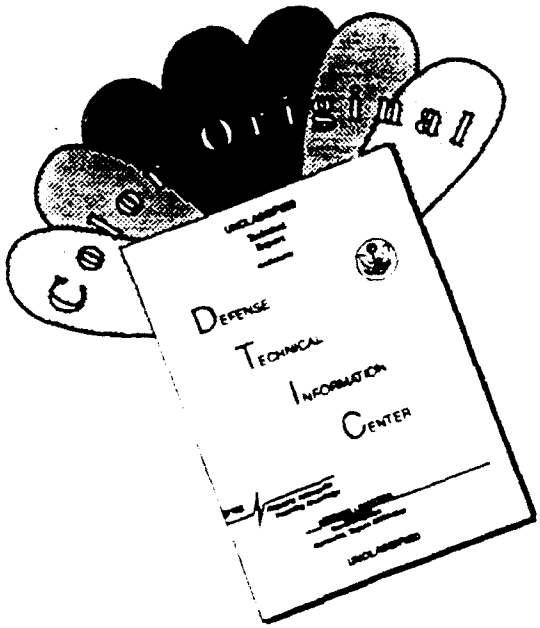

THIS DOCUMENT IS BEST QUALITY AVAILABLE. THE COPY FURNISHED TO DTIC CONTAINED A SIGNIFICANT NUMBER OF COLOR PAGES WHICH DO NOT REPRODUCE LEGIBLY ON BLACK AND WHITE MICROFICHE.

REPORT DOCUMENTATION PAGE

Form Approved
OMB No 0704-0188

1. AGENCY USE ONLY (Leave blank)	2. REPORT DATE	3. REPORT TYPE AND DATES COVERED
	March 1993	Final, Nov 90–Apr 91

4. TITLE AND SUBTITLE

The XNOVAKTC Rheological Model

5. FUNDING NUMBERS

PR: 1L161102AH43

6. AUTHOR(S)

Paul J. Conroy

7. PERFORMING ORGANIZATION NAME(S) AND ADDRESS(ES)

8. PERFORMING ORGANIZATION REPORT NUMBER

9. SPONSORING/MONITORING AGENCY NAME(S) AND ADDRESS(ES)

U.S. Army Research Laboratory
ATTN: AMSRL-OP-CI-B (Tech Lib)
Aberdeen Proving Ground, MD 21005-5066

10. SPONSORING/MONITORING AGENCY REPORT NUMBER

ARL-MR-47

11. SUPPLEMENTARY NOTES

12a. DISTRIBUTION/AVAILABILITY STATEMENT

Approved for public release; distribution is unlimited.

12b. DISTRIBUTION CODE

13. ABSTRACT *(Maximum 200 words)*

The rheological model, which is incorporated in the NOVA family of interior ballistic codes (Gough 1974), of which XNOVAKTC is the latest version, is examined in detail. The assumptions which are made in this model are also examined in detail. These assumptions are linked to the availability of experimental data, which may be used to guide constitutive modeling. Both empirical as well as analytical/experimental models are presented to provide the required mathematical closure of the solid-phase model. Previous work in this constitutive modeling area is discussed.

Interior ballistic simulations of realistic systems by XNOVAKTC are shown to predict values of intrinsic intergranular bed stress in excess of 100 MPa. However, available mixture stress vs. mixture density measurements have shown pronounced nonlinear behavior at values well below 100 MPa, which suggests that measurements are needed over a wider range of intrinsic stresses.

14. SUBJECT TERMS

interior ballistics, Navier Stokes equations, solid propellants, stress strain relations, solid phase, rheology

15. NUMBER OF PAGES

32

16. PRICE CODE

17. SECURITY CLASSIFICATION OF REPORT	18. SECURITY CLASSIFICATION OF THIS PAGE	19. SECURITY CLASSIFICATION OF ABSTRACT	20. LIMITATION OF ABSTRACT
UNCLASSIFIED	UNCLASSIFIED	UNCLASSIFIED	UL

INTENTIONALLY LEFT BLANK.

ACKNOWLEDGMENTS

The author wishes to acknowledge and express his appreciation for the support of his colleague Mr. Frederick W. Robbins, U.S. Army Research Laboratory (ARL), for checking and insuring the completeness of the derivation, as well as Dr. Douglas E. Kooker, ARL, for his continuing assistance in modeling solid-phase phenomena. Dr. Paul S. Gough's (Paul Gough Associates, Inc. (PGA)) comments and insightful explanations were also appreciated. Thanks must also go to Mr. Stowell Elder (BRL) who assisted in clarifying a dyadic.

(Note: The U.S. Army Ballistic Research Laboratory was deactivated on 30 September 1992 and subsequently became a part of the U.S. Army Research Laboratory (ARL) on 1 October 1992.)

INTENTIONALLY LEFT BLANK.

TABLE OF CONTENTS

INTENTIONALLY LEFT BLANK.

1. INTRODUCTION

This report examines Gough's (1974) derivation of the solid-phase portion of the Navier-Stokes equations of motion for the NOVA series of interior ballistic (IB) codes. The motivation for this report is the better understanding of the assumptions used in the formulation and how these may pertain to experimental data input for constitutive modeling. Also, this report provides the derivation in a concise location and step by step format for the unfamiliar reader.

2. DERIVATION OF THE CURRENT SOLID-PHASE EQUATIONS

The following is the derivation of the solid-phase Navier-Stokes equations for IB using the original formal averaging procedure used by Gough in 1974. Gough did not explicitly demonstrate this derivation of the solid-phase portion in his thesis. The more general, one-dimensional, isothermal Navier-Stokes equations include the solid-phase continuity equation,

$$\frac{\partial \rho_s}{\partial t} + \nabla \cdot (\rho_s \vec{u}_s) = \phi_s , \tag{1}$$

and solid-phase momentum equation,

$$\frac{\partial (\rho_s \vec{u}_s)}{\partial t} + \nabla \cdot (\rho_s \vec{u}_s \vec{u}_s + \bar{\bar{T}}_s) = \phi_s \vec{V}_s . \tag{2}$$

The principle assumptions to be made initially are: (1) that the propellant is compacted isothermally; (2) the stress tensor $\bar{\bar{T}}_s$ is macroscopically isotropic; and (3) the solid-phase mass production term is zero. The isothermal assumption considering the thermal scale, including combustion, assumes that the temperature rise of the propellant due to compaction is small with respect to the energy released by combustion. The isotropic assumption was made so the mixture stress (i.e., the intrinsic stress multiplied by the solid-phase volume fraction) could be more easily isolated from the gas pressure; this also eliminates any shear. The mass production is assumed zero over small time intervals due to the small production losses in comparison to the convective term.

Following the formal averaging procedure outlined in Gough's thesis, the momentum equation may be reduced through the following steps. No solid-phase mass production implies

$$\frac{\partial(\rho_s \vec{u}_s)}{\partial t} + \nabla \cdot (\rho_s \vec{u}_s \vec{u}_s + \vec{\vec{T}}_s) = 0. \tag{3}$$

Turbulent fluctuations of a variable are accounted for through the following typical notation, i.e.,

$$\rho_s = <\rho_s>^s + \rho_s^* \tag{4}$$

$$\vec{u}_s = <\vec{u}_s>^s + \vec{u}_s^* \tag{5}$$

and so on for other variables. Formal averaging may be written in either intrinsic (porosity weighted) or nonintrinsic forms,

$$<\rho_s(\vec{x},t)\vec{u}_s(\vec{x},t)\vec{u}_s(\vec{x},t) + \vec{\vec{T}}_s(\vec{x},t)>$$

$$= \varepsilon_s(\vec{x},t)<\rho_s(\vec{x},t)\vec{u}_s(\vec{x},t)\vec{u}_s(\vec{x},t) + \vec{\vec{T}}_s(\vec{x},t)>^s$$

or

$$= \int_{\mathcal{V}_s \tau_s} g(\vec{y} - \vec{x}, \tau - t)\left(\rho_s(\vec{y},\tau)\vec{u}_s(\vec{y},\tau)\vec{u}_s(\vec{y},\tau) + \vec{\vec{T}}_s(\vec{y},\tau)\right) dV d\tau \,. \tag{6}$$

The intrinsic average is identified by the term with the superscript s. Equation 6 introduces an arbitrary weighting function, g, which is assumed to be continuously differentiable and satisfies the normalization condition

$$\int_{-\infty}^{+\infty}\int_{-\infty}^{+\infty}\int_{-\infty}^{+\infty}\int_{-\infty}^{+\infty} g(\vec{y},\tau)\, dV d\tau = 1 \,. \tag{7}$$

Using

$$\frac{\partial\left(g(\vec{y} - \vec{x}, \tau - t)\right)}{\partial x_i} = -\frac{\partial\left(g(\vec{y} - \vec{x}, \tau - t)\right)}{\partial y_i} \,, \tag{8}$$

the development of the divergence term in Equation 3 may commence with the knowledge that ρ, $\vec{\vec{T}}$, and $\vec{u}$ are independent of the spacial dummy variable, y_i, allowing

$$\frac{\partial}{\partial x_i}<\rho_s(\vec{x},t)\vec{u}_s(\vec{x},t)\vec{u}_s(\vec{x},t) + \vec{\vec{T}}_s(\vec{x},t)>$$

$$= \int_{V_s}\int_{\tau_s} g(\vec{y}-\vec{x},\tau-t)\frac{\partial}{\partial y_i}\left(\rho_s(\vec{y},\tau)\vec{u}_s(\vec{y},\tau)\vec{u}_s(\vec{y},\tau) + \vec{\vec{T}}_s(\vec{y},\tau)\right)dVd\tau$$

$$- \int_{V_s}\int_{\tau_s}\frac{\partial}{\partial y_i}\left[g(\vec{y}-\vec{x},\tau-t)\left(\rho_s(\vec{y},\tau)\vec{u}_s(\vec{y},\tau)\vec{u}_s(\vec{y},\tau) + \vec{\vec{T}}_s(\vec{y},\tau)\right)\right]dVd\tau \ . \quad (9)$$

Using the definition of the nonintrinsic average and Gauss' theorem, both the divergence and temporal derivative terms of the momentum equation may be expanded as:

$$\frac{\partial}{\partial x_i}<\rho_s(\vec{x},t)\vec{u}_s(\vec{x},t)\vec{u}_s(\vec{x},t) + \vec{\vec{T}}_s(\vec{x},t)>$$

$$= <\frac{\partial}{\partial x_i}\left(\rho_s(\vec{x},t)\vec{u}_s(\vec{x},t)\vec{u}_s(\vec{x},t) + \vec{\vec{T}}_s(\vec{x},t)\right)>$$

$$- \int_{\sum_{sg}}\left(g(\vec{y}-\vec{x},\tau-t)\left(\rho_s(\vec{y},\tau)\vec{u}_s(\vec{y},\tau)\vec{u}_s(\vec{y},\tau) + \vec{\vec{T}}_s(\vec{y},\tau)\right)\right)\cdot\vec{n}dA \quad (10)$$

and

$$\frac{\partial}{\partial t}<\rho_s(\vec{x},t)\vec{u}_s(\vec{x},t)> = <\frac{\partial}{\partial t}\left(\rho_s(\vec{x},t)\vec{u}_s(\vec{x},t)\right)>$$

$$+ \int_{\sum_{sg}}\left(g(\vec{y}-\vec{x},\tau-t)\rho_s(\vec{y},\tau)\vec{u}_s(\vec{y},\tau)\right)\vec{w}\cdot\vec{n}dA \ , \quad (11)$$

where $\vec{w}$ is the relative velocity between the phases. The following nonintrinsic averaged form of the momentum equation may then be written using Equations 10 and 11,

$$\frac{\partial<\rho_s\vec{u}_s>}{\partial t} + \nabla\cdot\left(<\rho_s\vec{u}_s\vec{u}_s> + <\vec{\vec{T}}_s>\right) = -\int_{\sum_{sg}} g(\vec{\vec{T}}_s + \rho_s\vec{u}_s(\vec{u}_s-\vec{w}))\cdot\vec{n}dA \ . \quad (12)$$

Applying the intrinsic average to Equation 12 produces

$$\frac{\partial(\varepsilon_f<\rho_f\vec{u}_f>^f)}{\partial t} + \nabla\cdot\left(\varepsilon_f\left(<\rho_f\vec{u}_f\vec{u}_f>^f + <\vec{\tau}_f>^f\right)\right)$$

$$= -\int_{\Sigma_{fg}} g(\vec{\tau}_f + \rho_f\vec{u}_f(\vec{u}_f - \vec{w}))\cdot\vec{n}\,dA \qquad (13)$$

To further reduce the terms of this equation, one may write out the expansions for the averaging technique for products of two variables,

$$<\rho_f\vec{u}_f>^f = <\left(<\rho_f>^f + \rho_f^*\right)\left(<\vec{u}_f>^f + \vec{u}_f^*\right)>^f$$

$$= <\left(<\rho_f>^f<\vec{u}_f>^f + \rho_f^*<\vec{u}_f>^f + <\rho_f>^f\vec{u}_f^* + \rho_f^*\vec{u}_f^*\right)>^f \qquad (14)$$

and three variables,

$$<\rho_f\vec{u}_f\vec{u}_f>^f = <\left(<\rho_f>^f + \rho_f^*\right)\left(<\vec{u}_f>^f + \vec{u}_f^*\right)\left(<\vec{u}_f>^f + \vec{u}_f^*\right)>^f$$

$$= <\left(<\rho_f>^f<\vec{u}_f>^f + <\rho_f>^f\vec{u}_f^* + \rho_f^*<\vec{u}_f>^f + \rho_f^*\vec{u}_f^*\right)\left(<\vec{u}_f>^f + \vec{u}_f^*\right)>^f$$

$$= <(<\rho_f>^f<\vec{u}_f>^f<\vec{u}_f>^f + <\rho_f>^f\vec{u}_f^*<\vec{u}_f>^f + \rho_f^*<\vec{u}_f>^f<\vec{u}_f>^f + \rho_f^*\vec{u}_f^*<\vec{u}_f>^f$$

$$+ <\rho_f>^f<\vec{u}_f>^f\vec{u}_f^* + <\rho_f>^f\vec{u}_f^*\vec{u}_f^* + \rho_f^*<\vec{u}_f>^f\vec{u}_f^* + \rho_f^*\vec{u}_f^*\vec{u}_f^*)>^f \qquad (15)$$

The average of a fluctuating term alone, or the average of a fluctuating term multiplied by an averaged term, is zero, allowing the terms containing a single, averaged fluctuating variable to be neglected. The terms containing two or more fluctuating variables multiplied together and then averaged are not zero. It is also noted that the average of an averaged property is the average, that is,

$$<<\rho_s \vec{u}_s>^s> = <\rho_s \vec{u}_s>^s \tag{16}$$

This results in averaged momentum terms similar to Gough's equation (3.1.4.6),

$$<\rho_s \vec{u}_s>^s = <\rho_s>^s <\vec{u}_s>^s + <\rho_s^* \vec{u}_s^*>^s , \tag{17}$$

and equation (3.1.4.7),

$$<\rho_s \vec{u}_s \vec{u}_s>^s = <\rho_s>^s <\vec{u}_s>^s <\vec{u}_s>^s + <\rho_s>^s <\vec{u}_s^* \vec{u}_s^*>^s$$

$$+ 2<\vec{u}_s>^s <\rho_s^* \vec{u}_s^*>^s + <\rho_s^* \vec{u}_s^* \vec{u}_s^*>^s . \tag{18}$$

for the gas phase terms.

With this general background, the averaging of the momentum equation may proceed. The temporal term is expanded using Equation 17 as

$$\frac{\partial(\varepsilon_s <\rho_s \vec{u}_s>^s)}{\partial t} = <\vec{u}>^s \frac{\partial(\varepsilon_s <\rho_s>^s)}{\partial t} + \varepsilon_s <\rho_s>^s \frac{\partial <\vec{u}_s>^s}{\partial t} + \frac{\partial(\varepsilon_s <\rho^* \vec{u}^*>^s)}{\partial t} \tag{19}$$

The divergence term of Equation 12 expands to

$$\nabla \cdot \left(\varepsilon_s \left(<\rho_s \vec{u}_s \vec{u}_s>^s + <\vec{T}_s>^s\right)\right) = \nabla \cdot \left(\varepsilon_s \left(<\vec{T}_s>^s\right)\right)$$

$$+ \nabla \cdot \varepsilon_s \left(<\rho_s>^s <\vec{u}_s>^s <\vec{u}_s>^s + <\rho_s>^s <\vec{u}_s^* \vec{u}_s^*>^s \right.$$

$$\left. + 2<\vec{u}_s>^s <\rho_s^* \vec{u}_s^*>^s + <\rho_s^* \vec{u}_s^* \vec{u}_s^*>^s \right) . \tag{20}$$

Using the relation

$$\nabla \cdot (\vec{u}\,\vec{u}) = (\nabla \cdot \vec{u})\,\vec{u} + \vec{u} \cdot (\nabla\,\vec{u}), \tag{21}$$

which may be easily demonstrated in Cartesian coordinates for a well behaved vector $\vec{u}$, the expansion of the divergence term given in Equation 20 may then be written similar to Gough's equation (3.2.3.4) for the gas phase:

$$\begin{aligned}
\nabla \cdot \left(\varepsilon_g\left(<\rho_g \vec{u}_g \vec{u}_g>^g + <\vec{T}_g>^g\right)\right) &= \varepsilon_g <\rho^* \vec{u}^* \vec{u}^*>^g \cdot \nabla <\vec{u}_g>^g \\
&+ <\vec{u}_g>^g \nabla \cdot \left(\varepsilon_g <\rho_g>^g <\vec{u}_g>^g + \varepsilon_g <\rho^* \vec{u}^*>^g\right) \\
&+ \varepsilon_g <\rho_g>^g <\vec{u}_g>^g \cdot \nabla <\vec{u}_g>^g + \nabla \cdot \left(\varepsilon_g <\vec{T}_g>^g\right) \\
&+ \nabla \cdot \left(\varepsilon_g\left(<\rho_g>^g <\vec{u}^* \vec{u}^*>^g + <\vec{u}_g>^g <\rho^* \vec{u}^*>^g + <\rho^* \vec{u}^* \vec{u}^*>^g\right)\right)
\end{aligned} \tag{22}$$

With this and the temporal term in Equation 19 substituted into Equation 12, the momentum equation becomes

$$\begin{aligned}
&<\vec{u}_g>^g \frac{\partial(\varepsilon_g <\rho_g>^g)}{\partial t} + \varepsilon_g <\rho_g>^g \frac{\partial <\vec{u}_g>^g}{\partial t} + \frac{\partial(\varepsilon_g <\rho^* \vec{u}^*>^g)}{\partial t} \\
&+ \varepsilon_g <\rho^* \vec{u}^*>^g \cdot \nabla <\vec{u}_g>^g + <\vec{u}_g>^g \nabla \cdot \left(\varepsilon_g <\rho_g>^g <\vec{u}_g>^g + \varepsilon_g <\rho^* \vec{u}^*>^g\right) \\
&+ \varepsilon_g <\rho_g>^g <\vec{u}_g>^g \cdot \nabla <\vec{u}_g>^g + \nabla \cdot \left(\varepsilon_g <\vec{T}_g>^g\right) \\
&+ \nabla \cdot \left(\varepsilon_g\left(<\rho_g>^g <\vec{u}^* \vec{u}^*>^g + <\vec{u}_g>^g <\rho^* \vec{u}^*>^g + <\rho^* \vec{u}^* \vec{u}^*>^g\right)\right) \\
&= -\int_{\sum_g} g\left(\vec{T}_g + \rho_g \vec{u}_g (\vec{u}_g - \vec{w})\right) \cdot \vec{n}\, dA .
\end{aligned} \tag{23}$$

Similar operations with the restrictions of constant density, and nonreacting interfaces, transform the continuity equation (Equation 1) into

$$\frac{\partial(\varepsilon_s<\rho_s>^s)}{\partial t} + \nabla\cdot\varepsilon_s(<\rho_s>^s<\vec{u}_s>^s) = 0 . \tag{24}$$

Recognizing

$$\varepsilon_s<\rho_s>^s\frac{D<\vec{u}_s>^s}{Dt} = \varepsilon_s<\rho_s>^s\frac{\partial<\vec{u}_s>^s}{\partial t} + \varepsilon_s<\rho_s>^s\left(<\vec{u}_s>^s\cdot\nabla\right)<\vec{u}_s>^s \tag{25}$$

and applying Equation 24, with the assumption of no relative motion of the phases (i.e., $\vec{u}_s = \vec{u}_g$), to Equation 23 results in

$$\varepsilon_s<\rho_s>^s\frac{D<\vec{u}_s>^s}{Dt} + \nabla\cdot\left(\varepsilon_s<\bar{\bar{T}}_s>^s\right) = \theta_{2s} - \int_{\sum sg} g\,(\bar{\bar{T}}_s)\cdot\vec{n}dA , \tag{26}$$

where

$$\theta_{2s} = -\nabla\cdot\left(\varepsilon_s\left(<\rho_s>^s<\vec{u}^*_s,\vec{u}^*_s>^s\right)\right) . \tag{27}$$

Transformation of the unknown solid phase surface integral into a gas phase boundary condition may be accomplished by introducing an intrinsic intergranular stress describing the total stress on the propellant bed as

$$<\bar{\bar{T}}_s>^s = \bar{\bar{R}} + <\bar{\bar{T}}_g>^g , \tag{28}$$

where the gas phase contribution is considered as a hydrostatic pressure only

$$<\bar{\bar{T}}_g>^g = <P_g>^g\cdot\bar{\bar{I}} , \tag{29}$$

and the solid gas phase stress difference as

$$(\bar{\bar{T}}_s - \bar{\bar{T}}_g)\cdot\vec{n} = \vec{n}\Delta p , \tag{30}$$

where this interphase stress difference is usually zero unless the system is under reaction or surface tension. Using the following integral theorem for the averaged value of an intrinsic property,

$$\int_{V_g^i} \langle \bar{\bar{T}}_g \rangle^g \nabla\, g\, dV dt = -\nabla(\varepsilon_g \langle \bar{\bar{T}}_g \rangle^g) \,. \tag{31}$$

and applying Gauss' theorem to this provides

$$\int_{\sum sg} g \langle \bar{\bar{T}}_g \rangle^g \cdot \bar{n} dA = -\langle \bar{\bar{T}}_g \rangle^g \cdot \nabla \varepsilon_g \,. \tag{32}$$

thus allowing the integral term from Equation 26 to be written using Equations 30 and 32 as

$$\begin{aligned} \int_{\sum sg} g\, (\bar{\bar{T}}_s) \cdot \bar{n} dA = &- \langle \bar{\bar{T}}_g \rangle^g \cdot \nabla \varepsilon_g + \int_{\sum sg} g \left(\bar{\bar{T}}_g - \langle \bar{\bar{T}}_g \rangle^g \right) \cdot \bar{n} dA \\ &+ \int_{\sum sg} g\, (\Delta p) \cdot \bar{n} dA \,. \end{aligned} \tag{33}$$

The coupling stress integral on the left-hand side of Equation 33 is of both the averaged and fluctuating portion of the solid phase stress tensor. The first integral on the right-hand side of Equation 33 is merely the integral of the fluctuating portion of the gas phase stress tensor given by the relationship

$$\bar{\bar{T}}_g = \langle \bar{\bar{T}}_g \rangle^g + \bar{\bar{T}}_g^* \,. \tag{34}$$

Equation 26 may be rewritten using Equation 1 and the integral form of Equation 32, noting that there is a sign convention reversal of n for agreement with the gas phase, as

$$\begin{aligned} &\varepsilon_s \langle \rho_s \rangle^s \frac{D \langle \vec{u}_s \rangle^s}{Dt} + \nabla \cdot \left(\varepsilon_s \langle \bar{\bar{T}}_s \rangle^s \right) \\ &= \theta_{2s} - \langle \bar{\bar{T}}_g \rangle^g \cdot \nabla \varepsilon_g + \int_{\sum sg} g \bar{\bar{T}}_g^* \cdot \bar{n} dA - \Delta p \nabla \varepsilon_g \,. \end{aligned} \tag{35}$$

Using Equation 28 to expand the stress term and letting

$$\langle \rho_s \rangle^s = \rho_p \,, \tag{36}$$

results in

$$\varepsilon_s \langle \rho_s \rangle^s \frac{D \langle \vec{u}_s \rangle^s}{Dt} + \varepsilon_s \nabla \langle p_g \rangle^g + \nabla \cdot \left(\varepsilon_s \vec{R} \right)$$

$$= \theta_{2s} + \int_{\sum_{sg}} g \vec{T}_g^* \cdot \vec{n} dA - \Delta p \nabla \varepsilon_g \,. \tag{37}$$

where the subscript p denotes a property of the particle. The particle interfacial force term given by the integral on the right-hand side of Equation 37 is represented as

$$\int_{\sum_{sg}} g \vec{T}_g^* \cdot \vec{n} dA = \frac{\varepsilon_s \rho_p S_p}{m_p} \langle \vec{F} \rangle^i \,, \tag{38}$$

where $\langle F \rangle^i$ is the microscopic interaction, drag, between the media. Substituting this into Equation 35 results in the following form of the solid phase momentum equation:

$$\varepsilon_s \rho_p \frac{D \vec{u}_p}{Dt_p} + \varepsilon_s \nabla p_g + \nabla \cdot \left(\varepsilon_s \vec{R} \right) = \vec{f} \,. \tag{39}$$

where

$$\frac{D}{Dt_p} = \frac{\partial}{\partial t_p} + \vec{u}_p \cdot \nabla \tag{40}$$

and the interphase forces, as well as the turbulent momentum source term, are combined as

$$\vec{f} = \theta_{2s} + \frac{\varepsilon_s \rho_p S_p}{m_p} \langle \vec{F} \rangle^i - \Delta p \nabla \varepsilon_g \,. \tag{41}$$

Further manipulation of the averaged equations reformulates the momentum equation, after linearization of the stress term, into a recognizable wave equation as follows. The following averaged form of the solid phase continuity equation,

$$\rho_p \frac{\partial \varepsilon_s}{\partial t_p} + \rho_p \nabla \cdot \left(\varepsilon_s < \vec{u}_s >^s \right) = \dot{m} \ , \tag{42}$$

may be rewritten as

$$\rho_p \frac{D\varepsilon_s}{Dt_p} - \rho_p \varepsilon_s \nabla \cdot \vec{u}_p = \dot{m} \ , \tag{43}$$

where

$$\frac{D}{Dt_p} = \frac{\partial}{\partial t} + \vec{u}_p \cdot \nabla \ . \tag{44}$$

Expanding the stress term in the momentum Equation 39, with $\bar{\bar{R}}$ now represented as a hydrostatic stress,

$$\nabla (\varepsilon_s R) = \varepsilon_s \nabla R + R \nabla \varepsilon_s \ , \tag{45}$$

and further expanding the gradient term,

$$\nabla R = \frac{\partial R}{\partial \varepsilon_g} \nabla \varepsilon_g \ , \tag{46}$$

where the mixture stress of the particles is $\sigma_p = \varepsilon_s R$, provides

$$\nabla (\sigma_p) = \left(\varepsilon_s \frac{dR}{d\varepsilon_g} - R \right) \nabla \varepsilon_g \ . \tag{47}$$

Let $G(\varepsilon_s)$ be a compressive modulus such that

$$\nabla (\sigma_p) = G(\varepsilon_s) \nabla \varepsilon_g \ . \tag{48}$$

Substituting this into Equation 39 results in the following nonlinear momentum equation to be solved in the IB code

$$\varepsilon_s \rho_p \frac{D\vec{u}_p}{Dt_p} + \varepsilon_s \nabla p + G(\varepsilon_s) \nabla \varepsilon_g = \vec{f} \ . \tag{49}$$

Further assumptions are now made in order to model the stress term in the momentum equation. These assumptions consist of: [4] $f = 0$, no fluids in the propellant bed; [5] $u \cdot \nabla = 0$, the particles are initially at rest (i.e., for small perturbations about a quiescent state); and [6] $R = R(\varepsilon_g)$ only. The assumption of no fluid in the bed allows the gas pressure term to be neglected when computing the mixture stress. The small perturbations assumption eliminates the convective portion of the substantial derivative, thus the particles do not "flow," thus only accelerations and interaction forces exist. Assumption [6] is only for simplicity; of course, R is a function of temperature, contact surface area, and many other things which may or may not be experimentally measurable. The one variable that is measurable in a bed compaction test is the change in volume. This allows the computation of the porosity, assuming incompressibility or given the intrinsic equation of state of the particles from a second experiment.

Applying these assumptions reduces the momentum Equation 49 to

$$\varepsilon_{so} \rho_p \frac{\partial \vec{u}_p}{\partial t} + G_o(\varepsilon_{so}) \nabla \varepsilon_g = 0 \ , \tag{50}$$

and the continuity equation (Equation 1) to

$$\frac{\partial \varepsilon_s}{\partial t} = -\varepsilon_{so} \nabla \cdot \vec{u}_p \ . \tag{51}$$

One approach to deriving the solid phase wave speed is to take the derivative of the momentum equation with respect to time. The assumption that the intergranular stress R is not a function of time permits,

$$\varepsilon_{so} \rho_p \frac{\partial^2 \vec{u}_p}{\partial t^2} + G_o(\varepsilon_{so}) \frac{\partial}{\partial t} \nabla \varepsilon_g = 0 \ , \tag{52}$$

where

$$\frac{\partial}{\partial t}\nabla\varepsilon_g = \nabla\left(\frac{\partial\varepsilon_g}{\partial t}\right). \tag{53}$$

Using continuity equation (Equation 51), Equation 53 may be written as

$$\nabla\left(\frac{\partial\varepsilon_g}{\partial t}\right) = \nabla\left(\varepsilon_{so}\nabla\cdot\vec{u}_p\right), \tag{54}$$

which is

$$= \varepsilon_{so}\left(\nabla^2\vec{u}_p + \nabla\,\mathrm{curl}\,(\mathrm{curl}\,\vec{u}_p)\right). \tag{55}$$

Irrotational flow implies that the curl of the velocity is zero. Substituting this into the momentum equation, and dividing through by the porosity and density results in

$$\frac{\partial^2\vec{u}_p}{\partial t^2} + \frac{G_o(\varepsilon_{so})}{\rho_p}\nabla^2\vec{u}_p = 0. \tag{56}$$

This is a wave equation having a velocity of

$$a_{po}^2 = -\frac{G_o(\varepsilon_{so})}{\rho_p}, \tag{57}$$

where, for the linearized case,

$$G_o(\varepsilon_{so}) = \left[\varepsilon_{so}\frac{dR}{d\varepsilon_g} - R\right]. \tag{58}$$

In the general nonlinear case, the function G behaves as a "stiffness" modulus which is the product of the density and the propagation speed a_p^2,

$$G(\varepsilon_s) = \rho_p a_p^2. \tag{59}$$

3. RHEOLOGICAL REQUIREMENTS

In the theory underlying Gough's XNOVAKTC code (1990), the constitutive assumption which defines the solid-phase stress tensor is embedded into the function $G(\varepsilon_s)$ by specifying a functional dependence of the propagation speed a_p which is assigned for a system undergoing loading as

$$a_p = a_1 \frac{\varepsilon_{g_o}}{\varepsilon_g} , \tag{60}$$

and unloading

$$a_p = a_2 , \tag{61}$$

where the user-supplied constant a_1 represents the speed of propagation during compressive loading when the bed is at the settling porosity, ε_{so}, and the constant a_2 represents the propagation speed derived from the modulus during unloading from any state.

A functional dependance of $\sigma_p(\varepsilon_s)$ may be developed by rewriting Equation 50 as

$$\frac{d\sigma_p(\varepsilon_s)}{d\varepsilon_s} = G(\varepsilon_s) = -\frac{\rho_p}{g_o}\left(a_1 \frac{\varepsilon_{go}}{\varepsilon_g}\right)^2 = -\frac{d\sigma_p}{d\varepsilon_g} . \tag{62}$$

Integrating this relationship from ε_g to ε_{go}, where ε_g is the current gas phase porosity and ε_{go} is the settling porosity, and a_1 is the user-input propagation velocity of an infinitesimally small disturbance, generates the loading function used within the XNOVAKTC IB code,

$$\sigma_p(\varepsilon_g) = \frac{\rho_p a_1^2}{g_o}\varepsilon_{g_o}^2\left(\frac{1}{\varepsilon_g} - \frac{1}{\varepsilon_{g_o}}\right) . \tag{63}$$

Both a_1 and a_2 are experimentally determined constants. The speed of propagation of a small disturbance a_1^2 is usually about an order of magnitude smaller than that of a_2^2. These relations can be adjusted to the Robbins and Conroy (1991) model, which was performed on the data from the Birkett (1981) test rig as shown in Figure 1.

The four experimental data sets in Figure 1 end at different final force levels, while the functional data are plotted for four different disturbance propagation speeds, a_1, increasing from 100 m/s to 400 m/s from

the lower to the upper computed curve. ε_{go} is 0.45 and the diameter of the test cylinder was 7.62 cm. The curves shown in Figure 1 exhibit the correct trend. However, the chosen fixed wave speed does not represent the curving of the propellant experimental data as well as one might want.

The experiments which determine the user-input propagation velocity usually choose one value of the modulus from limited, typically below 1 MPa, axial stress levels. The data are obtained by compressing a bed of propellant in a cylinder and measuring the applied force and corresponding displacement. From this, a modulus, G, is determined at the settling porosity and then the simple relation

$$a_1 = \sqrt{\frac{G}{\rho_s}} \tag{64}$$

is used to obtain the compressional propagation speed for a small disturbance. Currently, only a limited amount of data is available for gun propellants of interest at this time (Conroy 1992). In addition, estimating the value of the modulus of the propellant involves a certain amount of ambiguity, because the 0.2% rule for determining the modulus is not applicable to a structure, such as a bed. Unfortunately, the predicted values of stress (particularly at small values of porosity, ε_g) are rather sensitive to the value of a_1 (as shown in Figure 1), which is dependent on the calculation of the modulus.

Class 3 HMX is a granular explosive with a settling porosity of 34.7%, whereas TS-3659 is a double-base ball propellant with a settling porosity of 40.0%. Figure 2 shows the region in which the propellant exhibits a stiffening behavior as the porosity decreases. Thus, to model the entire range of the propellant behavior, as potentially predicted in Figure 3 by the XNOVAKTC code, the experimental data should exceed the "knee" effect which typically occurs at a mixture stress (bed stress) of about 30 to 40 MPa for double-base propellants.

As a means of improving the current formulation, at least two approaches may be appropriate. The first, a direct correlation of experimental data, can produce the loading function for insertion into the code and thus a wave speed from the derivative thereof. Second, modeling of the bed aggregate from single grain behavior is more fundamental. In the past, modeling has been performed on various porous materials such as the elaborate spherical particle in the contact model of Brandt (1955) and the spherical pore collapse model (Carroll and Holt 1972). Brandt extends his work to include nonspherical particles continuing to apply Hertz's (1881) theory, which is valid as long as the particles have an average radius

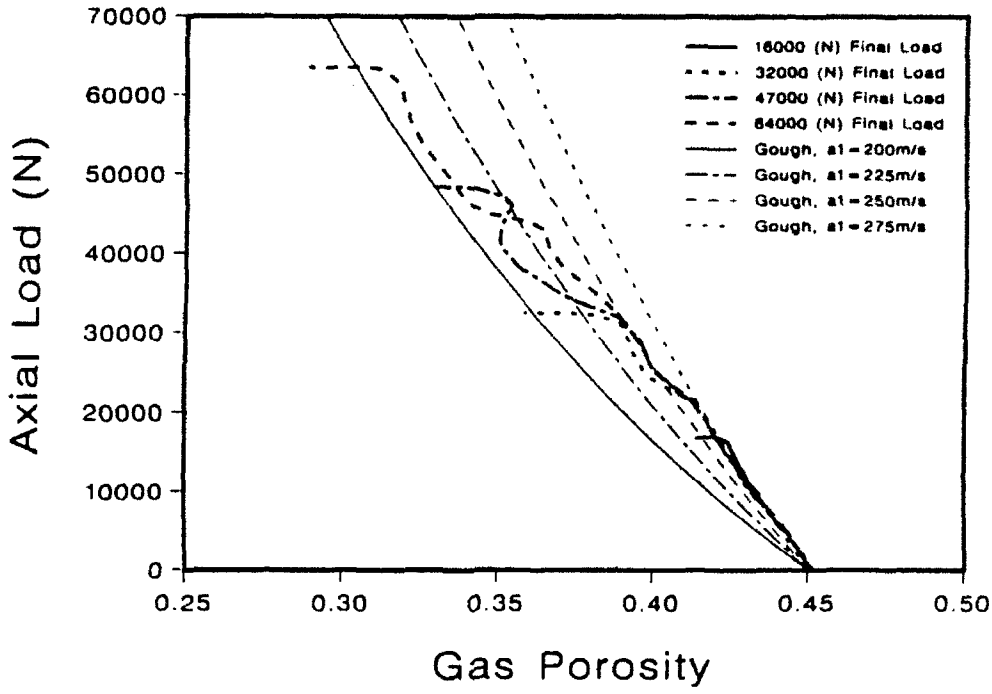

Figure 1. A comparison of axial load predictions given by Gough (equation 61) and the experimental data obtained at the Naval Ordnance Station (Birkett 1981) for M30 propellant at 219 K in a 3-in diameter compaction cylinder.

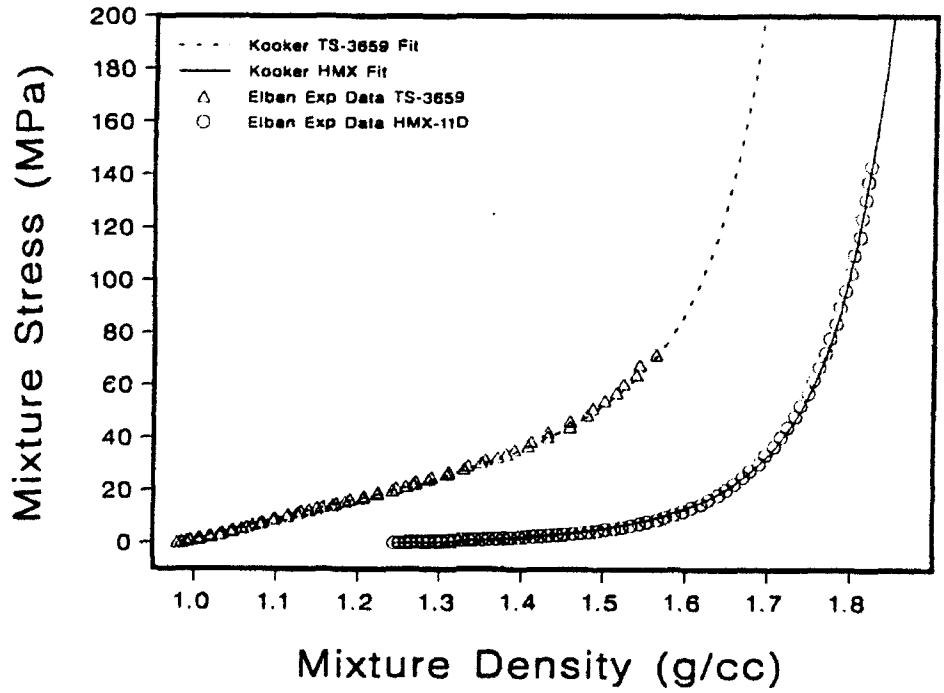

Figure 2. Experimental data for class 3 HMX and TS-3659 and Kooker's correlations.

The following page intentionally left blank.

INTENTIONALLY LEFT BLANK.

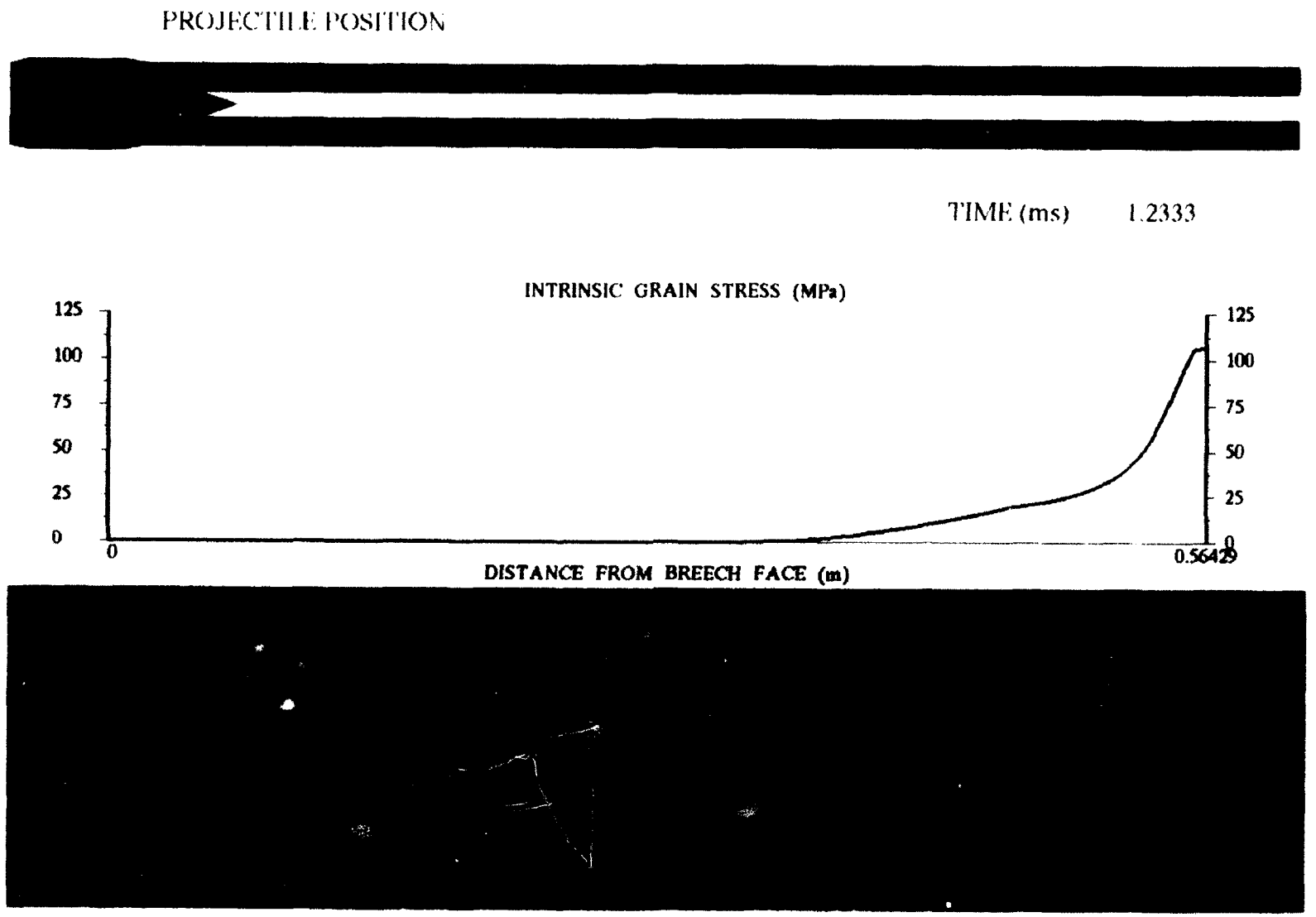

Figure 3. Axial distribution of grain stress, gas porosity, and gas velocity at 1.2 ms for a modified M829 120-mm tank charge.

The following page intentionally left blank

of curvature. There is some work on-going in this field for granular propellants at the ARL (Gazonas 1992), but is not otherwise being pursued to this author's knowledge. Costantino (1983) gave a review of the various models for energetic materials derived from rock mechanics.

A constitutive modeling comparison has been performed by Conroy and Kooker (1991). This report highlights Kooker's (Kooker and Anderson 1985) incorporation of the solid phase equation of state to model the compressibility and his correlation of experimental data, a modified from of Walton's (1977) equation. This was to demonstrate the potential prediction differences between the current model and one in which the data is correlated directly, currently isothermally. The results show some significant differences as Kooker's model tracks the solid material from the settling porosity to where it is a compressed solid with no voids.

4. DISCUSSION AND CONCLUSIONS

The formulation of the solid-phase portion of the current NOVA family of codes has been thoroughly described. The required closure for this portion of the IB model has been explained. Both analytical models, and analytical/experimental models have been examined by researchers as a means to provide the stress strain relationship needed by the derived solid-phase momentum equation. Previous investigators have resorted to using experimental propellant data to provide inputs for specific derived constitutive relationships from soil mechanics. The use of experimental data directly has also been investigated and is a viable and appropriate starting point for improving the current model, however, the data must be obtained in the regions to be investigated, which most probably will include the region above 100 MPa as presented in Figure 2. Noncoincidental efforts are currently underway to obtain quasi-static isothermal bed compaction data to 150 MPa for various propellants between BRL and Naval Surface Warfare Center, White Oak.

INTENTIONALLY LEFT BLANK.

5. REFERENCES

Birkett, J. A. "The Acquisition of M30A1 Propellant Rheology Data." Indian Head Technical Report, IHTR-724, Naval Ordnance Station Indian Head, MD, 30 September 1981.

Brandt, H. "A Study of the Speed of Sound in Porous Granular Media." Journal of Applied Mechanics, vol. 22, pp. 479–486, December 1955.

Carroll, M. M., and A. C. Holt. "Static and Dynamic Pore-Collapse Relations for Ductile Porous Materials." Journal of Applied Physics, vol. 43, no. 4, pp. 1627–1636, 1972.

Conroy, P. J. "Rheological Studies Related to Interior Ballistics: A Historical Perspective." BRL-MR-3970, U.S. Army Ballistic Research Laboratory, Aberdeen Proving Ground, MD, May 1992.

Conroy, P. J., and D. E. Kooker. "Implications of Gun Propellant Bed Rheology." Proceedings of the Fifth International Gun Propellant Symposium, U.S. Army Research, Development, and Engineering Center, Picatinny Arsenal, NJ, pp. 264–277, 19–21 November 1991.

Costantino, M. "The Relevance of Rock Mechanics to Gun Propellants." Proceedings of the 1983 JANNAF Structures and Mechanical Behavior Subcommittee Meeting, CPIA Publication 388, pp. 141–153, 1–3 November 1983.

Gazonas, G. A. Personal communication, February 1992.

Gough, P. S. "The Flow of a Compressible Gas Through an Aggregate of Mobile Reacting Particles." Ph.D. Thesis, Department of Mechanical Engineering, McGill University, Montreal, Quebec, December 1974.

Gough, P. S. "The XNOVAKTC Code." BRL-CR-627, U.S. Army Ballistic Research Laboratory, Aberdeen Proving Ground, MD, February 1990.

Hertz, H. Journal of Mathematics (Crelle's Journal), vol. 92, 1881.

Kooker, D. E., and R. D. Anderson. "Modeling of Hivelite Solid Propellant Combustion." BRL-TR-2649, U.S. Army Ballistic Research Laboratory, Aberdeen Proving Ground, MD, April 1985.

Robbins, F. W., and P. J. Conroy. "Rheological Studies of M30A1 Propellant." BRL-TR-3205, U.S. Army Ballistic Research Laboratory, Aberdeen Proving Ground, MD, February 1991.

Walton, O. R., et al. "Effects of Porosity, Strength, and Water Content on Attenuation of Stress Waves Generated by Subsurface Explosions in Soils." UCRL-79113, Lawrence Livermore National Laboratory, Livermore, CA, 1977.

INTENTIONALLY LEFT BLANK.

LIST OF SYMBOLS

A_1 = User input small disturbance propagation velocity

a = Compressional wave speed used in the solid phase wave equation

e_s = Solid phase internal energy

F = Microscopic interaction between the media

f = Interphase forces

f_s = Steady-state drag per unit volume

G = Bed modulus

G_o = Bed modulus at the settling porosity

g = Normalized weighting function used in averaging

$\bar{\bar{I}}$ = Identity matrix

$\dot{m}$ = Gas phase mass production per unit volume

P = Pressure

P_g = Gas phase pressure

P_s = Solid phase pressure

ΔP = Phase stress difference

q_s = Solid phase heat flux

R = Intergranular stress (hydrastatic)

$\bar{\bar{R}}$ = Intergranular stress tensor

r_b = Burning rate of the solid phase propellant

S_p = Interphase surface area

$\bar{\bar{T}}_s$ = Solid phase stress tensor

u_s = Solid phase velocity

V = Volume

V_s = External source velocity

w = Relative velocity between the phases

w_s = Interfacial velocity between the media

x = Position variable

y = Dummy variable of spacial integration

ϵ = Porosity

ε_g = Gas phase porosity

ε_o = Initial loading Porosity

ε_s = Solid phase porosity

ϕ_s = Solid phase mass generation

ρ_s = Solid phase density

σ_s = Bed mixture stress

θ_{2s} = Turbulent momentum source term

τ = Dummy variable of temporal integration

$_g$ = Subscript referring to the gas phase

$_s$ = Subscript referring to the solid phase

* = Superscript referring to the fluctuating portion of the variable

Σ_{sg} = Interfacial surface separating the phases

No. of Copies	Organization
2	Administrator Defense Technical Info Center ATTN: DTIC-DDA Cameron Station Alexandria, VA 22304-6145
1	Commander U.S. Army Materiel Command ATTN: AMCAM 5001 Eisenhower Ave. Alexandria, VA 22333-0001
1	Director U.S. Army Research Laboratory ATTN: AMSRL-D 2800 Powder Mill Rd. Adelphi, MD 20783-1145
1	Director U.S. Army Research Laboratory ATTN: AMSRL-OP-CI-AD, Tech Publishing 2800 Powder Mill Rd. Adelphi, MD 20783-1145
2	Commander U.S. Army Armament Research, Development, and Engineering Center ATTN: SMCAR-IMI-I Picatinny Arsenal, NJ 07806-5000
2	Commander U.S. Army Armament Research, Development, and Engineering Center ATTN: SMCAR-TDC Picatinny Arsenal, NJ 07806-5000
1	Director Benet Weapons Laboratory U.S. Army Armament Research, Development, and Engineering Center ATTN: SMCAR-CCB-TL Watervliet, NY 12189-4050
(Unclass. only) 1	Commander U.S. Army Rock Island Arsenal ATTN: SMCRI-IMC-RT/Technical Library Rock Island, IL 61299-5000
1	Director U.S. Army Aviation Research and Technology Activity ATTN: SAVRT-R (Library) M/S 219-3 Ames Research Center Moffett Field, CA 94035-1000

No. of Copies	Organization
1	Commander U.S. Army Missile Command ATTN: AMSMI-RD-CS-R (DOC) Redstone Arsenal, AL 35898-5010
1	Commander U.S. Army Tank-Automotive Command ATTN: ASQNC-TAC-DIT (Technical Information Center) Warren, MI 48397-5000
1	Director U.S. Army TRADOC Analysis Command ATTN: ATRC-WSR White Sands Missile Range, NM 88002-5502
1	Commandant U.S. Army Field Artillery School ATTN: ATSF-CSI Ft. Sill, OK 73503-5000
(Class. only) 1	Commandant U.S. Army Infantry School ATTN: ATSH-CD (Security Mgr.) Fort Benning, GA 31905-5660
(Unclass. only) 1	Commandant U.S. Army Infantry School ATTN: ATSH-CD-CSO-OR Fort Benning, GA 31905-5660
1	WL/MNOI Eglin AFB, FL 32542-5000
	Aberdeen Proving Ground
2	Dir, USAMSAA ATTN: AMXSY-D AMXSY-MP, H. Cohen
1	Cdr, USATECOM ATTN: AMSTE-TC
1	Dir, ERDEC ATTN: SCBRD-RT
1	Cdr, CBDA ATTN: AMSCB-CI
1	Dir, USARL ATTN: AMSRL-SL-I
10	Dir, USARL ATTN: AMSRL-OP-CI-B (Tech Lib)

No. of Copies	Organization
1	Chairman DOD Explosives Safety Board Room 856-C Hoffman Bldg. 1 2461 Eisenhower Avenue Alexandria, VA 22331-0600
1	Headquarters U.S. Army Materiel Command ATTN: AMCICP-AD, M. Fisette 5001 Eisenhower Ave. Alexandria, VA 22333-0001
1	U.S. Army Ballistic Missile Defense Systems Command Advanced Technology Center P.O. Box 1500 Huntsville, AL 35807-3801
1	Department of the Army Office of the Product Manager 155mm Howitzer, M109A6, Paladin ATTN: SFAE-AR-HIP-IP, Mr. R. De Kleine Picatinny Arsenal, NJ 07806-5000
3	Project Manager Advanced Field Artillery System ATTN: SFAE-ASM-AF-E LTC D. Ellis T. Kuriata J. Shields Picatinny Arsenal, NJ 07801-5000
1	Project Manager Advanced Field Artillery System ATTN: SFAE-ASM-AF-Q, W. Warren Picatinny Arsenal, NJ 07801-5000
2	Commander Production Base Modernization Agency U.S. Army Armament Research, Development, and Engineering Center ATTN: AMSMC-PBM, A. Siklosi AMSMC-PBM-E, L. Laibson Picatinny Arsenal, NJ 07806-5000
4	PEO-Armaments Project Manager Tank Main Armament System ATTN: AMCPM-TMA AMCPM-TMA-105 AMCPM-TMA-120 AMCPM-TMA-AS, H. Yuen Picatinny Arsenal, NJ 07806-5000
5	Commander U.S. Army Armament Research, Development, and Engineering Center ATTN: SMCAR-CCD, D. Spring SMCAR-CCH-V, C. Mandala E. Fennell SMCAR-CCH-T, L. Rosendorf SMCAR-CCS Picatinny Arsenal, NJ 07806-5000
19	Commander U.S. Army Armament Research, Development, and Engineering Center ATTN: SMCAR-AEE, J. Lannon SMCAR-AEE-B, A. Beardell D. Downs S. Einstein S. Westley S. Bernstein J. Rutkowski B. Brodman P. O'Reilly R. Cirincione A. Grabowsky P. Hui J. O'Reilly SMCAR-AEE-WW, M. Mezger J. Pinto D. Wiegand P. Lu C. Hu SMCAR-AES, S. Kaplowitz Picatinny Arsenal, NJ 07806-5000
1	Commander U.S. Army Armament Research, Development and Engineering Center ATTN: SMCAR-HFM, E. Barrieres Picatinny Arsenal, NJ 07806-5000

No. of Copies	Organization
9	Commander U.S. Army Armament Research, Development and Engineering Center ATTN: SMCAR-FSA-T, M. Salsbury SMCAR-FSA-F, LTC R. Riddle SMCAR-FSC, G. Ferdinand SMCAR-FS, T. Gora SMCAR-FS-DH, J. Feneck SMCAR-FSS-A, R. Kopman B. Machek L. Pinder SMCAR-FSN-N, K. Chung Picatinny Arsenal, NJ 07806-5000
3	Director Benet Weapons Laboratories ATTN: SMCAR-CCB-RA, G.P. O'Hara G.A. Pflegl SMCAR-CCB-S, F. Heiser Watervliet, NY 12189-4050
2	Commander U.S. Army Research Office ATTN: Technical Library D. Mann P.O. Box 12211 Research Triangle Park, NC 27709-2211
1	Commander, USACECOM R&D Technical Library ATTN: ASQNC-ELC-IS-L-R, Myer Center Fort Monmouth, NJ 07703-5301
1	Commander U.S. Army Harry Diamond Laboratory ATTN: SLCHD-TA-L 2800 Powder Mill Rd. Adelphi, MD 20783-1145
1	Commandant U.S. Army Aviation School ATTN: Aviation Agency Fort Rucker, AL 36360
1	Program Manager U.S. Tank-Automotive Command ATTN: AMCPM-ABMS, T. Dean Warren, MI 48092-2498

No. of Copies	Organization
1	Project Manager U.S. Tank-Automotive Command Fighting Vehicle Systems ATTN: SFAE-ASM-BV Warren, MI 48397-5000
1	Project Manager, Abrams Tank System ATTN: SFAE-ASM-AB Warren, MI 48397-5000
1	Director HQ, TRAC RPD ATTN: ATCD-MA Fort Monroe, VA 23651-5143
2	Director U.S. Army Materials Technology Laboratory ATTN: SLCMT-ATL (2 cps) Watertown, MA 02172-0001
1	Commander U.S. Army Belvoir Research and Development Center ATTN: STRBE-WC Fort Belvoir, VA 22060-5006
1	Director U.S. Army TRAC-Ft. Lee ATTN: ATRC-L, Mr. Cameron Fort Lee, VA 23801-6140
1	Commandant U.S. Army Command and General Staff College Fort Leavenworth, KS 66027
1	Commandant U.S. Army Special Warfare School ATTN: Rev and Trng Lit Div Fort Bragg, NC 28307
1	Commander Radford Army Ammunition Plant ATTN: SMCAR-QA/HI LIB Radford, VA 24141-0298

No. of Copies	Organization
1	Commander U.S. Army Foreign Science and Technology Center ATTN: AMXST-MC-3 220 Seventh Street, NE Charlottesville, VA 22901-5396
2	Commandant U.S. Army Field Artillery Center and School ATTN: ATSF-CO-MW, E. Dublisky ATSF-CN, P. Gross Ft. Sill, OK 73503-5600
1	Commandant U.S. Army Armor School ATTN: ATZK-CD-MS, M. Falkovitch Armor Agency Fort Knox, KY 40121-5215
1	U.S. Army European Research Office ATTN: Dr. Roy E. Richenbach Box 65 FPO New York 09510-1500
2	Commander Naval Sea Systems Command ATTN: SEA 62R SEA 64 Washington, DC 20362-5101
1	Commander Naval Air Systems Command ATTN: AIR-954-Tech Library Washington, DC 20360
4	Commander Naval Research Laboratory ATTN: Technical Library Code 4410, K. Kailasanate J. Boris E. Oran Washington, DC 20375-5000
1	Office of Naval Research ATTN: Code 473, R.S. Miller 800 N. Quincy Street Arlington, VA 22217-9999
1	Office of Naval Technology ATTN: ONT-213, D. Siegel 800 N. Quincy St. Arlington, VA 22217-5000

No. of Copies	Organization
4	Commander Naval Surface Warfare Center ATTN: Code 730 Code R-13, R. Bernecker H. Sandusky Silver Spring, MD 20903-5000
7	Commander Naval Surface Warfare Center ATTN: T.C. Smith K. Rice S. Mitchell S. Peters J. Consaga C. Gotzmer Technical Library Indian Head, MD 20640-5000
5	Commander Naval Surface Warfare Center ATTN: Code G30, Code G32, Code G33, J.L. East T. Doran Code E23 Technical Library Dahlgren, VA 22448-5000
5	Commander Naval Air Warfare Center ATTN: Code 388, C.F. Price T. Boggs Code 3895, T. Parr R. Derr Information Science Division China Lake, CA 93555-6001
1	Commanding Officer Naval Underwater Systems Center ATTN: Code 5B331, Technical Library Newport, RI 02840
1	AFOSR/NA ATTN: J. Tishkoff Bolling AFB, D.C. 20332-6448
1	OLAC PL/TSTL ATTN: D. Shiplett Edwards AFB, CA 93523-5000

No. of Copies Organization

3 AL/LSCF
ATTN: J. Levine
L. Quinn
T. Edwards
Edwards AFB, CA 93523-5000

1 WL/MNAA
ATTN: B. Simpson
Eglin AFB, FL 32542-5434

1 WL/MNME
Energetic Materials Branch
2306 Perimeter Rd.
STE 9
Eglin AFB, FL 32542-5910

1 WL/MNSH
ATTN: R. Drabczuk
Eglin AFB, FL 32542-5434

2 NASA Langley Research Center
ATTN: M.S. 408, W. Scallion
D. Witcofski
Hampton, VA 23605

1 Central Intelligence Agency
Office of the Central References
Dissemination Branch
Room GE-47, HQS
Washington, DC 20502

1 Central Intelligence Agency
ATTN: J. Backofen
NHB, Room 5N01
Washington, DC 20505

1 SDIO/TNI
ATTN: L.H. Caveny
Pentagon
Washington, DC 20301-7100

1 SDIO/DA
ATTN: E. Gerry
Pentagon
Washington, DC 21301-7100

2 HQ DNA
ATTN: D. Lewis
A. Fahey
6801 Telegraph Rd.
Alexandria, VA 22310-3398

No. of Copies Organization

1 Director
Sandia National Laboratories
Energetic Materials & Fluid Mechanics
Department, 1512
ATTN: M. Baer
P.O. Box 5800
Albuquerque, NM 87185

1 Director
Sandia National Laboratories
Combustion Research Facility
ATTN: R. Carling
Livermore, CA 94551-0469

4 Director
Lawrence Livermore National
Laboratory
ATTN: L-355,
A. Buckingham
G. Benedetti
M. Finger
L-324, M. Constantino
P.O. Box 808
Livermore, CA 94550-0622

2 Director
Los Alamos Scientific Lab
ATTN: T3/D. Butler
M. Division/B. Craig
P.O. Box 1663
Los Alamos, NM 87544

2 Battelle Columbus Laboratories
ATTN: TACTEC Library, J.N. Huggins
V. Levin
505 King Avenue
Columbus, OH 43201-2693

1 Battelle PNL
ATTN: Mr. Mark Garnich
P.O. Box 999
Richland, WA 99352

1 Institute of Gas Technology
ATTN: D. Gidaspow
3424 S. State Street
Chicago, IL 60616-3896

1 Institute for Advanced Technology
ATTN: T.M. Krehne
The University of Texas of Austin
4030-2 W. Braker Lane
Austin, TX 78759-5329

No. of Copies	Organization
2	CPIA - JHU ATTN: Hary J. Hoffman T. Christian 10630 Little Patuxent Parkway Suite 202 Columbia, MD 21044-3200
1	Brigham Young University Department of Chemical Engineering ATTN: M. Beckstead Provo, UT 84601
1	Jet Propulsion Laboratory California Institute of Technology ATTN: L.D. Strand, MS 125/224 4800 Oak Grove Drive Pasadena, CA 91109
1	California Institute of Technology 204 Karman Lab Main Stop 301-46 ATTN: F.E.C. Culick 1201 E. California Street Pasadena, CA 91109
3	Georgia Institute of Technology School of Aerospace Engineering ATTN: B.T. Zim E. Price W.C. Strahle Atlanta, GA 30332
1	Massachusetts Institute of Technology Department of Mechanical Engineering ATTN: T. Toong 77 Massachusetts Avenue Cambridge, MA 02139-4307
2	University of Illinois Department of Mechanical/Industry Engineering ATTN: H. Krier R. Beddini 144 MEB; 1206 N. Green St. Urbana, IL 61801-2978
1	University of Maryland ATTN: Dr. J.D. Anderson College Park, MD 20740

No. of Copies	Organization
1	University of Massachusetts Department of Mechanical Engineering ATTN: K. Jakus Amherst, MA 01002-0014
1	University of Minnesota Department of Mechanical Engineering ATTN: E. Fletcher Minneapolis, MN 55414-3368
3	Pennsylvania State University Department of Mechanical Engineering ATTN: V. Yang K. Kuo C. Merkle University Park, PA 16802-7501
1	Rensselaer Polytechnic Institute Department of Mathematics Troy, NY 12181
1	Stevens Institute of Technology Davidson Laboratory ATTN: R. McAlevy III Castle Point Station Hoboken, NJ 07030-5907
1	Rutgers University Department of Mechanical and Aerospace Engineering ATTN: S. Temkin University Heights Campus New Brunswick, NJ 08903
1	University of Southern California Mechanical Engineering Department ATTN: 0HE200, M. Gerstein Los Angeles, CA 90089-5199
1	University of Utah Department of Chemical Engineering ATTN: A. Baer Salt Lake City, UT 84112-1194
1	Washington State University Department of Mechanical Engineering ATTN: C.T. Crowe Pullman, WA 99163-5201
1	AFELM, The Rand Corporation ATTN: Library D 1700 Main Street Santa Monica, CA 90401-3297

No. of Copies	Organization
1	Arrow Technology Associates, Inc. ATTN: W. Hathaway P.O. Box 4218 South Burlington, VT 05401-0042
3	AAI Corporation ATTN: J. Hebert J. Frankle D. Cleveland P.O. Box 126 Hunt Valley, MD 21030-0126
2	Alliant Techsystems, Inc. ATTN: R.E. Tompkins J. Kennedy 7225 Northland Dr. Brooklyn Park, MN 55428
1	AVCO Everett Research Laboratory ATTN: D. Stickler 2385 Revere Beach Parkway Everett, MA 02149-5936
1	General Applied Sciences Lab ATTN: J. Erdos 77 Raynor Ave. Ronkonkama, NY 11779-6649
1	General Electric Company Tactical System Department ATTN: J. Mandzy 100 Plastics Ave. Pittsfield, MA 01201-3698
1	IITRI ATTN: M.J. Klein 10 W. 35th Street Chicago, IL 60616-3799
4	Hercules, Inc. Radford Army Ammunition Plant ATTN: L. Gizzi D.A. Worrell W.J. Worrell C. Chandler Radford, VA 24141-0299
2	Hercules, Inc. Allegheny Ballistics Laboratory ATTN: William B. Walkup Thomas F. Farabaugh P.O. Box 210 Rocket Center, WV 26726

No. of Copies	Organization
1	Hercules, Inc. Aerospace ATTN: R. Cartwright 100 Howard Blvd. Kenville, NJ 07847
1	Hercules, Inc. Hercules Plaza ATTN: B.M. Riggleman Wilmington, DE 19894
1	MBR Research Inc. ATTN: Dr. Moshe Ben-Reuven 601 Ewing St., Suite C-22 Princeton, NJ 08540
1	Olin Corporation Badger Army Ammunition Plant ATTN: F.E. Wolf Baraboo, WI 53913
3	Olin Ordnance ATTN: E.J. Kirschke A.F. Gonzalez D.W. Worthington P.O. Box 222 St. Marks, FL 32355-0222
1	Olin Ordnance ATTN: H.A. McElroy 10101 9th Street, North St. Petersburg, FL 33716
1	Paul Gough Associates, Inc. ATTN: P.S. Gough 1048 South St. Portsmouth, NH 03801-5423
1	Physics International Library ATTN: H. Wayne Wampler P.O. Box 5010 San Leandro, CA 94577-0599
2	Princeton Combustion Research Laboratories, Inc. ATTN: N. Mer N.A. Messina Princeton Corporate Plaza 11 Deerpark Dr., Bldg IV, Suite 119 Monmouth Junction, NJ 08852

No. of Copies	Organization
3	Rockwell International Rocketdyne Division ATTN: BA08, J. Flanagan J. Gray R.B. Edelman 6633 Canoga Avenue Canoga Park, CA 91303-2703
2	Rockwell International Science Center ATTN: Dr. S. Chakravarthy Dr. S. Palaniswamy 1049 Camino Dos Rios P.O. Box 1085 Thousand Oaks, CA 91360
1	Southwest Research Institute ATTN: J.P. Riegel 6220 Culebra Road P.O. Drawer 28510 San Antonio, TX 78228-0510
1	Sverdrup Technology, Inc. ATTN: Dr. John Deur 2001 Aerospace Parkway Brook Park, OH 44142
3	Thiokol Corporation Elkton Division ATTN: R. Willer R. Biddle Tech Library P.O. Box 241 Elkton, MD 21921-0241
1	Veritay Technology, Inc. ATTN: E. Fisher 4845 Millersport Hwy. East Amherst, NY 14501-0305
1	Universal Propulsion Company ATTN: H.J. McSpadden 25401 North Central Ave. Phoenix, AZ 85027-7837
1	SRI International Propulsion Sciences Division ATTN: Tech Library 333 Ravenwood Avenue Menlo Park, CA 94025-3493
	Aberdeen Proving Ground
1	Cdr, USACSTA ATTN: STECS-PO/R. Hendricksen

No. of
Copies Organization

1 Ernst-Mach-Institut
ATTN: Dr. R. Heiser
Haupstrasse 18
Weil am Rheim
Germany

1 Defence Research Agency, Military Division
ATTN: C. Woodley
RARDE Fort Halstead
Sevenoaks, Kent, TN14 7BP
England

1 School of Mechanical, Materials, and Civil Engineering
ATTN: Dr. Bryan Lawton
Royal Military College of Science
Shrivenham, Swindon, Wiltshire, SN6 8LA
England

No. of
Copies Organization

2 Institut Saint Louis
ATTN: Dr. Marc Giraud
Dr. Gunther Sheets
Postfach 1260
7858 Weail am Rhein 1
Germany

1 Explosive Ordnance Division
ATTN: A. Wildegger-Gaissmaier
Defence Science and Technology Organisation
P.O. Box 1750
Salisbury, South Australia 5108

1 Armaments Division
ATTN: Dr. J. Lavigne
Defence Research Establishment Valcartier
2459, Pie XI Blvd., North
P.O. Box 8800
Courcelette, Quebec G0A 1R0
Canada

INTENTIONALLY LEFT BLANK.

USER EVALUATION SHEET/CHANGE OF ADDRESS

This Laboratory undertakes a continuing effort to improve the quality of the reports it publishes. Your comments/answers to the items/questions below will aid us in our efforts.

1. ARL Report Number ARL-MR-47 Date of Report March 1993

2. Date Report Received _____

3. Does this report satisfy a need? (Comment on purpose, related project, or other area of interest for which the report will be used.) _____

4. Specifically, how is the report being used? (Information source, design data, procedure, source of ideas, etc.) _____

5. Has the information in this report led to any quantitative savings as far as man-hours or dollars saved, operating costs avoided, or efficiencies achieved, etc? If so, please elaborate _____

6. General Comments. What do you think should be changed to improve future reports? (Indicate changes to organization, technical content, format, etc.) _____

CURRENT ADDRESS

_____
Organization

_____
Name

_____
Street or P.O. Box No.

_____
City, State, Zip Code

7. If indicating a Change of Address or Address Correction, please provide the Current or Correct address above and the Old or Incorrect address below.

OLD ADDRESS

_____
Organization

_____
Name

_____
Street or P.O. Box No.

_____
City, State, Zip Code

(Remove this sheet, fold as indicated, staple or tape closed, and mail.)

DEPARTMENT OF THE ARMY

OFFICIAL BUSINESS

BUSINESS REPLY MAIL
FIRST CLASS PERMIT No 0001, APG, MD

Postage will be paid by addressee

Director
U.S. Army Research Laboratory
ATTN: AMSRL-OP-CI-B (Tech Lib)
Aberdeen Proving Ground, MD 21005-5066

NO POSTAGE
NECESSARY
IF MAILED
IN THE
UNITED STATES